國 立 中 央 大 學

物 理 學 系
碩 士 論 文

Time Evolution of the Holographic Entanglement Entropy from Black Hole Thermalization

研 究 生：孫柏鈞
指導教授：陳江梅

中 華 民 國　一一〇　年　六　月

Time Evolution of the Holographic Entanglement Entropy from Black Hole Thermalization

A dissertation submitted in partial fulfillment
of the requirements for the degree of

Master of Science in Physics

at the

NATIONAL CENTRAL UNIVERSITY,
CHUNGLI 32001, TAIWAN.

June 2021

Author .....

Po-Chun Sun
Department of Physics

Certified by .....

Professor Chiang-Mei Chen
Thesis Supervisor

Accepted by .....

Professor Wen-Yu Wen
Thesis Committee

Professor Yi-Zen Chu
Thesis Committee

國立中央大學圖書館學位論文授權書

填單日期：2021 / 6 / 30　　2019.9 版

授權人姓名	孫柏鈞	學 號	108222031
系所名稱	物理學系	學位類別	☑碩士　□博士
論文名稱	Time Evolution of the Holographic Entanglement Entropy from Black Hole Thermalization	指導教授	陳江梅

學位論文網路公開授權

授權本人撰寫之學位論文全文電子檔：

- 在「**國立中央大學圖書館博碩士論文系統**」.
  - (✓)同意立即網路公開
  - (　)同意 於西元＿＿＿年＿月＿日網路公開
  - (　)不同意網路公開，原因是：＿＿＿＿＿＿＿＿＿＿
- 在**國家圖書館「臺灣博碩士論文知識加值系統」**
  - (✓)同意立即網路公開
  - (　)同意 於西元＿＿＿年＿月＿日網路公開
  - (　)不同意網路公開，原因是：＿＿＿＿＿＿＿＿＿＿

依著作權法規定，非專屬、無償授權國立中央大學、台灣聯合大學系統與國家圖書館，不限地域、時間與次數，以文件、錄影帶、錄音帶、光碟、微縮、數位化或其他方式將上列授權標的基於非營利目的進行重製。

學位論文紙本延後公開申請 (紙本學位論文**立即公開者此欄免填**)

本人撰寫之學位論文紙本因以下原因將延後公開

- **延後原因**
  - (　)已申請專利並檢附證明，專利申請案號：
  - (　)準備以上列論文投稿期刊
  - (　)涉國家機密
  - (　)依法不得提供，請說明：＿＿＿＿＿＿＿＿
- **公開日期**：西元＿＿＿＿年＿＿＿＿月＿＿＿＿日

※繳交教務處註冊組之紙本論文(送繳國家圖書館)若不立即公開，請加填「國家圖書館學位論文延後公開申請書」

研究生簽名：孫柏鈞　　指導教授簽名：陳江梅

國立中央大學碩士班研究生

論文指導教授推薦書

物理 學系/研究所 孫柏鈞 研究生所提之論文 Time Evolution of the Holographic Entanglement Entropy from Black Hole Thermalization 係由本人指導撰述，同意提付審查。

指導教授 孫以均 (簽章)

2021 年 6 月 10 日

104.07.24

National Central University

Verification Letter from the Oral Examination Committee

for Master's Students

This thesis titled

Time Evolution of the Holographic Entanglement Entropy from Black Hole Thermalization

is written by Po-Chun Sun (孫柏鈞) studying in the graduate program in Physics. The author of this thesis is qualified for a master's degree through the verification of the committee.

Convener of the Degree Examination Committee

溫之弘

Members

Date: 2021/06/29

(YYYY/MM/DD)

1090326

摘要

我們藉由全像原理，考慮Hartle–Hawking 狀態下，$(n+1)$維度的永恆黑洞在反德西特空間(AdS)偶合到具有保角對稱的熱庫(CFT reservoir)，來研究霍金輻射的糾纏熵在$(n+1)$維的Kerr-Newman黑洞蒸發的過程隨時間演化。試想保角熱庫對偶到$(n+2)$維重力空間，而原本我們所考慮的$(n+1)$維度的反德西特空間黑洞被嵌入在高一維的流形，則此情況完全可以用Randall–Sundrum模型來描述。

根據島規則 [1]，糾纏熵在半古典重力可以分爲來自量子效應與重力的貢獻。其中量子效應可以用Ryu–Takayanagi公式來得到，而重力部分等於量子極面(quantum extremal surface)除以四倍的牛頓常數。我們展示了在此全像系統演化晚期，糾纏熵成長是線性的。過了佩吉時間(Page time)，量子極面出現並且系統達到飽和。在這篇論文中，我們將強調在任意維度的時空，黑洞旋轉如何如何引響其糾纏熵。

Key Words: 全像理論、反德西特/共形場論對偶、霍金粒子、糾纏熵、量子極面、黑洞資訊悖論

Abstract

We study the time evolution of the entanglement entropy of Hawking radiation in the $(n+1)-$dimensional Kerr-Newman black hole evaporation by the holographic approach that considering the $(n+1)-$dimensional AdS eternal black brane coupled to the auxiliary CFT reservoir is in the Hartle-Hawking state. The CFT reservoir itself has a holographic dual, the $(n+2)-$dimensional bulk geometry, and the original $(n+1)-$dimensional AdS-black brane is embedded into such bulk manifold, which is precisely Randall–Sundrum model.

According to the island rule [1], the entanglement entropy in semi-classical gravity can be divided into two parts, one is due to the quantum effects, which can be obtained by Ryu–Takayanagi conjecture. Another is the gravitational part, which is equal to the area of the quantum extremal surface divided by four times the Newton's constant. We show that the entanglement growth in our holographic system is linear in late times. After Page time, the system reaches saturation since the entanglement islands appear. In this thesis, we will emphasize how black hole rotation affects entanglement entropy in general dimensional spacetime.

Key Words: Holography, AdS/CFT, Hawking Radiation, Entanglement Entropy, Quantum Extremal Island, Information Paradox

Acknowledgements

I am very grateful to my teacher and the guys from our meeting group for the weekly journal club. All of the discussions during the meeting is valuable for me.

Contents

List of Figures

Chapter 1

Introduction

Quantum mechanics is a fundamental theory that tremendous success at the microscopic level. On the other hand, general relativity is a useful theory of gravitation that passes many experiment tests. Nevertheless, from the combination of two theories, the black hole information paradox is a big conundrum for decades. Let's illustrate that with an explicit example. Starting from a star in pure state collapses to form a black hole, and then some entangled pairs are created near the event horizon such that those particles go out the black hole entangled with the particles inside the black hole. It is turn out to be a mixed state when the black hole completely evaporates, which contradicts the time evolution symmetry (the whole system is unitary) according to quantum mechanics.

1.1 Holographic Entanglement Entropy

Before going to the resolution of information loss, we need to talk about entanglement entropy. Entanglement is a quantum measurement with non-local property, which plays an important role in quantum information. Considering a quantum system which can be divided into two parts, Σ and Σ^c, such that the total Hilbert space is a direct product of these two subsystems as $H_{\text{tot}} = H_\Sigma \otimes H_{\Sigma^c}$. For a quantum state $|\Psi\rangle \in H_{\text{tot}}$, the reduced density matrix of Σ is defined, by tracing out the degree of freedom of subsystem Σ^c, as $\rho_\Sigma = \text{Tr}_{\Sigma^c}(|\Psi\rangle\langle\Psi|)$. Then the entanglement entropy of Σ is defined as

$$\mathcal{S}_A \equiv -\text{Tr}(\rho_\Sigma \ln \rho_\Sigma), \tag{1.1}$$

which is the measurement to describe the correlation between Σ and Σ^c.

Recently, there is a glimmer of hope for the black hole information paradox that has been discovered by the holographic principle. The holographic principle [2,3] has successfully connected two very different theories: gravity in the bulk and quantum field theory (QFT) on the boundary, which state that all of the information in the bulk manifold is encoded in QFT lives in the boundary. The implication can be observed by regarding the black hole as ordinary quantum mechanics object. Think about the

system in the region Σ, from the quantum statistical perspective, the entropy of the system $\mathcal{S}_\Sigma = -\operatorname{Tr}\rho\ln\rho$ can be obtained by calculating the density matrix ρ for Σ. Therefore, the maximal entropy of the system with $\mathcal{N}-$dimensional Hilbert space is $\mathcal{S}_{\Sigma,max} = \ln\mathcal{N}$. Alongside this, once we recognize the entropy of the system cannot greater than the Bekenstein-Hawking entropy of the black hole with the black hole area $A = \partial\Sigma$, we conclude the number of degree of freedom of any quantum gravity system Σ is bounded by the area $A = \partial\Sigma$ $i.e.$

$$\ln\mathcal{N} \leq \frac{A}{4G_N^{(\Sigma)}} = \frac{A}{4\ell_p^2}\,. \tag{1.2}$$

One of the famous examples is the AdS/CFT correspondence [4–6]. In this framework, Ryu and Takanayagi proposed that the entanglement entropy in QFT between the spatial region Σ and its outside can be computed from the RT formula [7, 8]

$$\mathcal{S}_\Sigma = \frac{\mathcal{A}_\Gamma}{4G_N}, \tag{1.3}$$

where $\mathcal{A}_\Gamma$ is the area of the extremal surface (with the minimal area) in the bulk that the end of which is connected to the entangled surface. The Ryu-Takayanagi proposal provides a very different and, in many situations, convenient approach to study entanglement entropy. The calculations of the holographic entanglement entropy(HEE) in vacuum were firstly carried out in [7, 8]. The references [9–11] provide nice reviews about studying entanglement entropy by the holographic method. Although the entanglement entropy is very different from the thermal entropy, people have been analyzed the thermodynamics of entanglement entropy in the thermal state by exploring the HEE of black holes in the small R limit [12–19]. Moreover, it has been proved that the extremal surface cannot penetrate the horizon in static black holes [20] which implies that in the large R limit, the area of the extremal surface will be dominated by the IR region after regularization because a great part of the extremal surface runs along the event horizon. One can expect that, after regularization, the leading behavior of the area of the extremal surface in the large R limit is identical to Bekenstein-Hawking entropy, thermal entropy. There are some discussions of the entanglement entropy in the large R limit [14–19, 21]. All of the above examples are the cases that the HEE in static spacetime, and the generalization of time-dependent proposal (HRT formula) is worked by [22]. People have been interesting to see the thermalization processes [23–26] underlying the HRT proposal. If the bulk gravitational system is coupled to quantum matter, the von Neumann (fine-grained) entropy also can be calculated in semi-classical limit by extremizing the quantum extremal surface [27, 28].

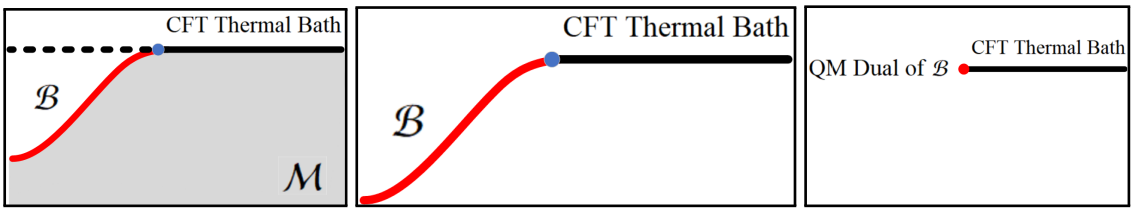

Figure 1.1: The $\mathcal{M}$ is the $(n+2)-$dimensional bulk manifold and the $\mathcal{B}$ is the $(n+1)-$dimensional Plank brane. *Left*: bulk perspective; *Middle*: brane perspective; *Right*: boundary perspective.

1.2 Entanglement Entropy of Hawking Radiation

The papers [29, 30] show that the entanglement entropy increases at early times in the system, the black hole is evaporated by adding an auxiliary quantum thermal bath (the black hole with a thermal bath in the Hartle-Hawking state), and the entanglement entropy decreases in late times owing to the appearance of the quantum extremal island, which leads to the reconstruction of the entanglement wedges. [1] provides a new way to think about such $(n+1)-$dimensional gravitational system add quantum matters couple to a thermal bath. There are three different alternative descriptions:

1. Bulk Perspective: describing the quantum matters as more than one dimension gravitational dual (bulk manifold). The original $n-$dimensional gravitational system lives on the dynamical brane (Planck brane), and the Planck brane is embedded in the bulk manifold.

2. Brane Perspective: the ordinary picture which we have described.

3. Boundary Perspective: describing the gravitational part as less than one dimension QFT dual.

Apart from that, let's say Υ is the radiation region in the quantum reservoir, then, according to the island rule is proposed by [1], the von Neumann entropy in semi-classical approximation can be computed by

$$\mathcal{S}_{\Upsilon} = Min\left\{ \underset{\mathcal{I}}{Ext}\left[\mathcal{S}^{(\text{eff})}_{QFT}(\Upsilon \cup \mathcal{I}) + \frac{\mathcal{A}_{\partial\mathcal{I}}}{4G_N^{(brane)}} \right] \right\} . \tag{1.4}$$

where the corresponding reduced density $\rho^{(\text{eff})}_{\Upsilon\cup\mathcal{I}}$ in semi-classical limit is different from the reduced density $\rho_{\Upsilon\cup\mathcal{I}}$ in the exact quantum theory. Hence, the metric we consider in this thesis is always classical gravity. Using the RT formula (1.3), we can calculate the entanglement entropy in QFT by $\mathcal{S}^{(\text{eff})}_{QFT}(\Upsilon \cup \mathcal{I}) = \frac{\mathcal{A}_{\Gamma}}{4G_N^{(bulk)}}$ where Γ is the RT surface that homologous to Υ. There is an explicit computation of time evolution of entanglement entropy and quantum extremal island to resolve the information paradox for two-dimensional AdS black hole in equilibrium (eternal black hole) with a thermal bath in [31]. The papers [32–35] demonstrate that, even in the higher dimension, the

resolution is worked. Here we need to emphasize that although there is a new prediction that quantum extremal surface appears due to holography, we do not know how Hawking particles bring out the information, what the mechanism is such that the quantum extremal surface looks like a screen. Also, there is an ambiguity how radiation regions increase.

In this thesis, we generalize the previous work from [33] to rotating black hole. To simulate the rotating charged black hole in real world, we employ the time evolution of von Neumann entropy in the system, the $(n+1)-$dimensional AdS-Kerr-Newman black hole, with the planar horizon, in equilibrium with a CFT bath in the Hartle-Hawking state. We analytically calculate the fine-grained entropy in the case that the brane with weak tension limit, which means its backreaction to the bulk geometry is negligible. Before Page time, there is no island $\mathcal{I} = \{\emptyset\}$, the RT surface Γ across the bulk horizon. Hence, Γ is equal to the wormhole path (Einstein–Rosen bridges). The entanglement entropy increase because the area of the wormhole increase with time [36]. Particularly, in late times, the entanglement entropy grows linearly because of the stretching of space inside the horizon [37]. There is no intersection between the entanglement wedges of Hawking radiation and Planck branes until Page time. After Page time, the system reaches saturation and $\mathcal{I} \neq \{\emptyset\}$, the RT surface Γ across the Planck brane, the RT surface Γ is equivalent to the minimal surface defect in which given strip in $(n-1)-$dimensional spatial region. Due to the reconstruction of the entanglement wedges, there is an intersection between entanglement wedges of Hawking radiation and Planck branes. On top of that, the saturation entropy in the weak tension limit is closed to Bekenstein-Hawking entropy.

1.3 Cylindrical Kerr-Newman Black Brane

Let's discuss some properties of cylindrical Kerr-Newman black hole. Consider an observer moves with the velocity $v = a/\Theta$ in $(n+2)$-dimensional charged AdS-black branes, that is, Lorentz boost along the spatial direction ϕ

$$dt \;\rightarrow\; \Theta\, dt - a\, d\phi, \qquad d\phi \;\rightarrow\; \Theta\, d\phi - a\, dt, \tag{1.5}$$

where $a \in (-\infty, \infty)$ is a rotating parameter when the spatial coordinate ϕ is identified as $\phi \sim \phi + 2\pi$ and $\Theta = \sqrt{1+a^2}$. The line element of a cylindrical Kerr-Newman black brane becomes [38]

$$ds^2 = \frac{L^2}{z^2}\left[-h(z)(\Theta\, dt - a\, d\phi)^2 + \frac{dz^2}{h(z)} + (\Theta\, d\phi - a\, dt)^2 + d\sigma_{n-1}^2\right], \tag{1.6}$$

where $d\sigma_{n-1}^2$ is the line element of $(n-1)$-dimensional Euclidean space and the emblackening function is

$$h(z) = 1 - mz^{n+1} + q^2 z^{2n}, \tag{1.7}$$

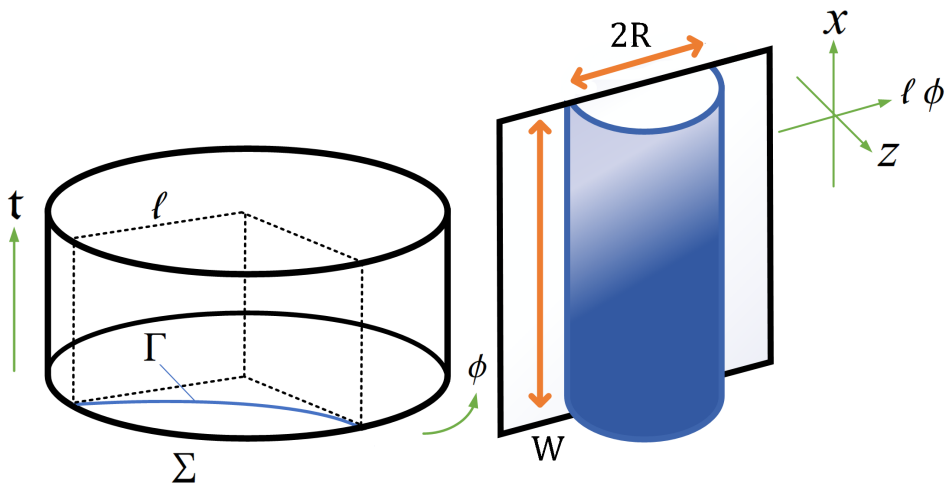

Figure 1.2: *Left*: The global structure of $(n+2)-$dimensional cylindrical spacetime. ℓ is the radius of the cylinder, Σ is the considered spatial region, Γ_Σ is the extremal surface (blue curve) for the spatial region Σ. *Right*: The extremal surface in $(n+1)-$dimensional spatial slice for Σ is a strip.

including mass and charge parameters. The associated gauge potential is

$$A = \sqrt{\frac{n}{2(n-1)}}\, q\, (z_h^{n-1} - z^{n-1})(\Theta\, dt - a\, d\phi). \tag{1.8}$$

By integrating the flux of $\mathcal{F}^{\mu\nu}$ on the boundary of the spacelike hypersurface, we get the density of electromagnetic charge [39]

$$\mathcal{Q} = \frac{q\Theta}{4\pi G_N} \frac{n(n-1)}{2} \tag{1.9}$$

The time-like Killing vector ∂_t corresponds to the conserved quantity, namely the energy density

$$\mathcal{E} = \frac{m}{16\pi G_N} \left[(n+1)\Theta^2 - 1\right], \tag{1.10}$$

and the Killing vector along the azimuthal direction ∂_ϕ implies the conservation of angular momentum. The angular momentum density is

$$\mathcal{J} = \frac{n+1}{16\pi G_N}\, m\, a\, \Theta. \tag{1.11}$$

According to the definition of the horizon, $h(z_h) = 0$, we can express mass in terms of horizon radius z_h

$$m = \frac{q^2 z_h^{2n} + 1}{z_h^{n+1}}. \tag{1.12}$$

For fixed m, there are two corresponding horizons, the inner and outer horizons, for the non-extreme case. However, the top of the extremal surface, z_b, cannot greater than the outer event horizon, so we consider z_h as the radius of the outer horizon in the

following context. Therefore, we can rewrite the emblackening function (1.7) as

$$h(z) = 1 - g(z), \qquad g(z) = \frac{z^{n+1}}{z_h^{n+1}} + q^2 z^{n+1} \left(z_h^{n-1} - z^{n-1} \right). \tag{1.13}$$

The temperature of the black brane (1.6) is

$$T = -\frac{h'(z_h)}{4\pi\Theta} = \frac{n+1}{4\pi\Theta z_h} \left(1 - \frac{n-1}{n+1} q^2 z_h^{2n} \right). \tag{1.14}$$

There is an upper bound of charge parameter

$$q \leq \sqrt{\frac{n+1}{n-1}} \frac{1}{z_h^n}, \tag{1.15}$$

which ensures the non-negative temperature $T \geq 0$. The equality holds when the black brane is extremal. In addition, the electromagnetic field in bulk geometry corresponds to the chemical potential of the field theory on the boundary

$$\mu = \lim_{z \to 0} A_t(z) = \sqrt{\frac{n}{2(n-1)}}\, q\, \Theta\, z_h^{n-1}. \tag{1.16}$$

Thus, we can write the HEE in terms of chemical potential and temperature [17].

The organization of this thesis as follows. In chapter 2, we build up our doubly-holographic system and illustrate how to embed the Planck brane into the bulk manifold. In chapter 3, we write down the general formula for the time evolution of wormhole area, evaluating entanglement velocity at late times. Furthermore, we calculate the entanglement entropy when quantum extremal islands appear in chapter 4. In the end, we summarize some important results and discuss some physics meaning in chapter 5. We put the detailed calculations of HEE in cylindrical Kerr-Newman black hole in Appendix A.

Chapter 2

Holography Setup

In the paper [7], the framework is underline AdS/CFT, which is that the pure quantum mechanical system dual to the pure gravitational system. Now we study the gravitational system with the quantum matter, and the quantum part has the gravitational dual. We do not know what the precise density matrix ρ is in such quantum gravity, and it is doable in semi-classical gravity because the metric is still classical. Although it may not be a good approximation, hope it gives some clues about quantum gravity and the resolution of information paradox.

2.1 Review AdS/BCFT

We consider the AdS/BCFT correspondence [40, 41], denoting $(\mathcal{M}, \mathfrak{g})$ as the $(n+2)-$dimensional bulk manifold and $(\mathcal{B}, \mathfrak{h})$ as the $(n+1)-$dimensional brane manifold in the bulk, the action can be written as

$$I = I_{\mathcal{M}} + I_{\mathcal{B}} \tag{2.1}$$

where

$$I_{\mathcal{M}} \equiv \frac{1}{16\pi G_N^{(n+2)}} \int_{\mathcal{M}} d^{n+2}x\sqrt{|\mathfrak{g}|}\,(R - 2\Lambda) - \int_{\mathcal{M}} d^{n+2}x\sqrt{|\mathfrak{g}|}\frac{\mathcal{F}^2}{4}\,, \tag{2.2}$$

$$I_{\mathcal{B}} \equiv \frac{1}{8\pi G_N^{(n+2)}} \int_{\mathcal{B}} d^{n+1}x\sqrt{|\mathfrak{h}|}\,(K - \mathcal{T}_{\mathcal{B}})\,, \quad K = \mathfrak{h}^{ij}K_{ij}\,. \tag{2.3}$$

The quantity R is the Ricci scalar, $\Lambda = -\frac{n(n+1)}{2L^2}$ is the cosmological constant with the AdS_{n+2} radius L, $\mathcal{F}_{\mu\nu}$ is the electromagnetic tensor, K_{ij} is the extrinsic curvature and $\mathcal{T}_{\mathcal{B}}$ is the tension on the brane $\mathcal{B}$. By varying the bulk action (2.2) with respect to bulk metric $\mathfrak{g}_{\mu\nu}$ and the gauge vector of electromagnetic tensor $\mathcal{A}_\mu$, we get the equation of motion on $\mathcal{M}$ is

$$R_{\mu\nu} + \frac{n+1}{L^2}\mathfrak{g}_{\mu\nu} = 8\pi G_N^{(n+2)}\left(T_{\mu\nu} - \frac{T}{n}\mathfrak{g}_{\mu\nu}\right) \tag{2.4}$$

where

$$T_{\mu\nu} = \mathcal{F}_{\mu\alpha}\mathcal{F}_{\nu}{}^{\alpha} - \frac{\mathcal{F}^2}{4}\mathfrak{g}_{\mu\nu}\,, \qquad \nabla_\mu \mathcal{F}^{\mu\nu} = 0 \tag{2.5}$$

and $T = \mathfrak{g}^{\mu\nu}T_{\mu\nu}$. By imposing the Neumann boundary condition on $\mathcal{B}$ ($i.e.\ \delta\mathfrak{h}_{ij} \neq 0$), we obtain the equation of motion on $\mathcal{B}$ [42] is

$$K_{ij} - K\mathfrak{h}_{ij} + \mathcal{T}_{\mathcal{B}}\mathfrak{h}_{ij} = 0 \tag{2.6}$$

with the constraint

$$n^\mu \mathcal{F}_{\mu\nu} P^{\nu}{}_{j} = 0 \tag{2.7}$$

where n^μ is the unit vector normal to brane and $P^{\nu}{}_{j}$ is the projection tensor.

2.2 Black Brane Thermalization

Recall the expectation of an observable in a thermal state (grand canonical ensemble) can be calculated by $\langle\mathcal{O}\rangle_T = \frac{1}{Z}\mathrm{Tr}\left(\mathcal{O}e^{-\beta(H-\mu\mathcal{Q}+\Omega\mathcal{J})}\right) = \mathrm{Tr}\left(\mathcal{O}\rho_T\right)$ in which $\rho_T = \frac{1}{Z}\sum_n e^{-\beta(H-\mu\mathcal{Q}+\Omega\mathcal{J})}\left|\psi_n\right\rangle\left\langle\psi_n\right|$ is the density matrix and Z is the partition function. There is another idea to think about the QFT at finite temperature [43]. Consider the total Hilbert space can be written as two copies of the system $H_{tot} = H_L \otimes H_R$ and prepare a special entangled state, the thermofield double (TFD) state

$$\left|\Psi\right\rangle = \frac{1}{\sqrt{Z}}\sum_n e^{-\beta(H-\mu\mathcal{Q}+\Omega\mathcal{J})/2}\left|\psi_n\right\rangle_L \otimes \left|\psi_n\right\rangle_R\,. \tag{2.8}$$

Notice that the state (2.8) is invariant under $H_R - H_L$. We see that the reduced density matrix for subsystem H_R is $\rho_R = \mathrm{Tr}_L\left(\left|\Psi\right\rangle\left\langle\Psi\right|\right) = \frac{1}{Z}\sum_n e^{-\beta(H-\mu\mathcal{Q}+\Omega\mathcal{J})}\left|\psi_n\right\rangle_R{}_R\langle\psi_n|$, which is the same as the thermal density matrix ρ_T. Hence we can interpret the emergence of temperature owing to the ignorance of the subsystem H_L.

For bulk perspective, we take the $\mathbb{Z}_2$ quotient [34] across the brane in the bulk manifold $\mathcal{M}$. To evaluate the von Neumann entropy of the Radiation region, according to the island rule (1.4), we need to compare the no island phase and island phase, and then choose the minimal one

$$\mathcal{S}_\Upsilon = Min\left\{\frac{\mathcal{A}_{\Gamma,\mathcal{I}=\{\emptyset\}}}{4G_N^{(\mathcal{M})}},\ \underset{\mathcal{I}\neq\{\emptyset\}}{Ext}\left[\frac{\mathcal{A}_\Gamma}{4G_N^{(\mathcal{M})}} + \frac{\mathcal{A}_{\partial\mathcal{I}}}{4G_N^{(\mathcal{B})}}\right]\right\}\,. \tag{2.9}$$

Our consideration of the system is the following: for $\mathfrak{t} < 0$, the CFT reservoir and the AdS-black brane on $\mathcal{B}$ are decoupled ($i.e.$ imposing the reflecting boundary conditions on the boundary of $\mathcal{B}$); at $\mathfrak{t}$=0, the CFT reservoir and the AdS-black brane are coupled and the black brane on $\mathcal{B}$ start evaporating but fixing the temperature. At Page time, quantum extremal surfaces appear and the entanglement entropy stops increasing.

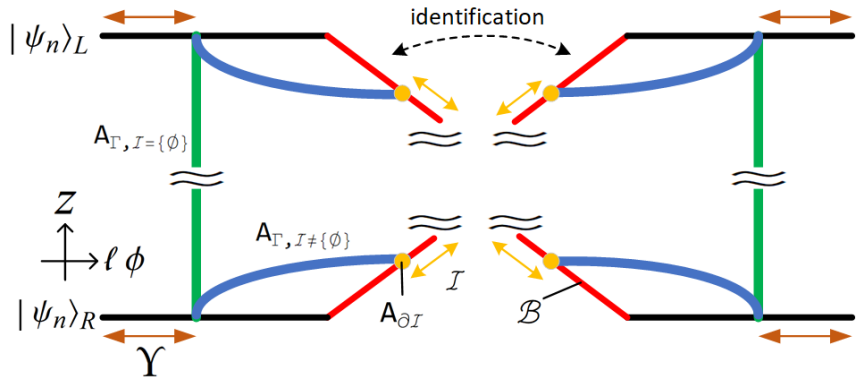

Figure 2.1: The black line is the CFT reservoir; the red line represents the Plank brane $\mathcal{B}$ where the islands $\mathcal{I} \subseteq \mathcal{B}$ appear after Page time. The yellow dots are the quantum extremal surface which are the boundary of the islands $\partial\mathcal{I} = \mathcal{B} \cap \Gamma$. Before Page time, the RT surface Γ is the green line. After Page time, the RT surface transit from the green line to the blue line.

2.3 Induced Gravity on Planck Brane

Our goal is to derive a way to embed the $(n+1)-$dimensional Kerr-Newman black brane into the $(n+2)-$dimensional asymptotically Kerr-Newman black brane. In this subsection, we will analytically show how to embed the AdS_{n+1} into AdS_{n+2}, that is, the Hartle-Hawking state on pure AdS with zero temperature auxiliary reservoir. In the general case, the $(n+1)-$dimensional AdS black brane on $\mathcal{B}$ with finite temperature thermal bath, the bulk geometry $\mathcal{M}$ is difficult to write down analytically, but [32] provides a nice way to numerically construct the bulk geometry by using the Deturck trick. Especially, the bulk geometry become exact AdS black brane while we consider weak tension limit on $\mathcal{B}$.

2.3.1 AdS on the Brane

Start from the AdS foliated metric

$$ds^2_{AdS_{n+2}} = \frac{L^2}{\sin^2\theta}\left(d\theta^2 + \frac{ds^2_{AdS_{n+1}}}{L^2}\right) \tag{2.10}$$

$$= \frac{L^2}{z^2}\left(-dt^2 + dz^2 + \ell^2 d\phi^2 + d\sigma^2_{n-1}\right) . \tag{2.11}$$

Later we will consider the cylindrical rotating black brane as the bulk, the length ℓ is the radius of the cylinder and the coordinate ϕ is compactified as $\phi \sim \phi + 2\pi$. To simplify our notation, we let ℓ to be 1. Let's say the brane is located at $\theta = \theta_{\mathcal{B}}$, then the induced metric on $\mathcal{B}$ is

$$ds^2_{\mathcal{B}} = \frac{L^2_{\mathcal{B}}}{\omega^2}\left(-dt^2 + d\omega^2 + d\sigma^2_{n-1}\right) . \tag{2.12}$$

Note that we have the following relations:

$$z = \omega \sin\theta, \quad \phi = \omega \cos\theta \,. \tag{2.13}$$

By the Israel junction condition (2.6), we are able to compute the tension on $\mathcal{B}$

$$\mathcal{T}_{\mathcal{B}} = \frac{n}{L}\cos\theta_{\mathcal{B}} \,. \tag{2.14}$$

From (2.10), (2.12) and (2.14), it is easy to read off that the length scale $L_{\mathcal{B}}$ on brane is

$$\frac{1}{L_{\mathcal{B}}^2} = \frac{\sin^2\theta_{\mathcal{B}}}{L^2} = \frac{1}{L^2}\left(1 - \frac{L^2\mathcal{T}_{\mathcal{B}}}{n^2}\right) \,. \tag{2.15}$$

2.3.2 Black Hole on the Brane

Instead of directly solving (2.4), we deal with the modified equation [32]

$$R_{\mu\nu} + \frac{n+1}{L^2}\mathfrak{g}_{\mu\nu} = 8\pi G_N^{(n+2)}\left(T_{\mu\nu} - \frac{T}{n}\mathfrak{g}_{\mu\nu}\right) + \nabla_{(\mu}\xi_{\nu)} \tag{2.16}$$

where $\xi^\mu \equiv \left[\Gamma^\mu_{\alpha\beta}(\mathfrak{g}) - \Gamma^\mu_{\alpha\beta}(\tilde{\mathfrak{g}})\right]\mathfrak{g}^{\alpha\beta}$ is the Deturck vector and $\tilde{\mathfrak{g}}$ is the reference metric in which the boundary conditions are identical to $\mathfrak{g}$ on Dirichlet boundaries. More explicitly, the corresponding line element of the reference metric $\tilde{\mathfrak{g}}$ is

$$ds^2_{\widetilde{\mathcal{M}}} = \frac{L^2}{z^2}\left(-h(z)(\Theta\, dt - a\, d\phi)^2 + \frac{dz^2}{h(z)} + (\Theta\, d\phi - a\, dt)^2 + d\sigma^2_{n-1}\right) \tag{2.17}$$

where $h(z)$ is the emblackening factor of the black brane. Let's say $w = z\cot\theta + \phi$ and the brane $\mathcal{B}$ is situated at $w = 0$ and the bulk geometry only takes the part $w \geq 0$. For the numerical purpose, it is convenient to introduce the new dimensionless variables,

$$x = \frac{w}{w+1} \quad \text{and} \quad y = \sqrt{1 - \frac{z}{z_h}} \,. \tag{2.18}$$

We follow [32] to present the general metric ansatz

$$ds^2_{\mathcal{M}} = \frac{L^2}{(1-y^2)^2 z_h^2}\Bigg\{ - h(y)K_1\left[\Theta dt - aK_5\left(\frac{dx}{(1-x)^2} + 2z_h K_3\, y\, dy\right)\right]^2 + \frac{4z_h^2 K_2\, y^2 dy^2}{h(y)} \tag{2.19}$$

$$+ K_4\left[\Theta\left(\frac{dx}{(1-x)^2} + 2z_h K_3\, y\, dy\right) - aK_6\, dt\right]^2 + K_7\, d\sigma^2_{n-1}\Bigg\} \tag{2.20}$$

with the emblackening factor

$$h(y) = 1 - g(y), \quad g(z) = (1-y^2)^{n+1}\left[1 + q^2 z_h^{2n}\left(1 - (1-y^2)^{n-1}\right)\right] \,. \tag{2.21}$$

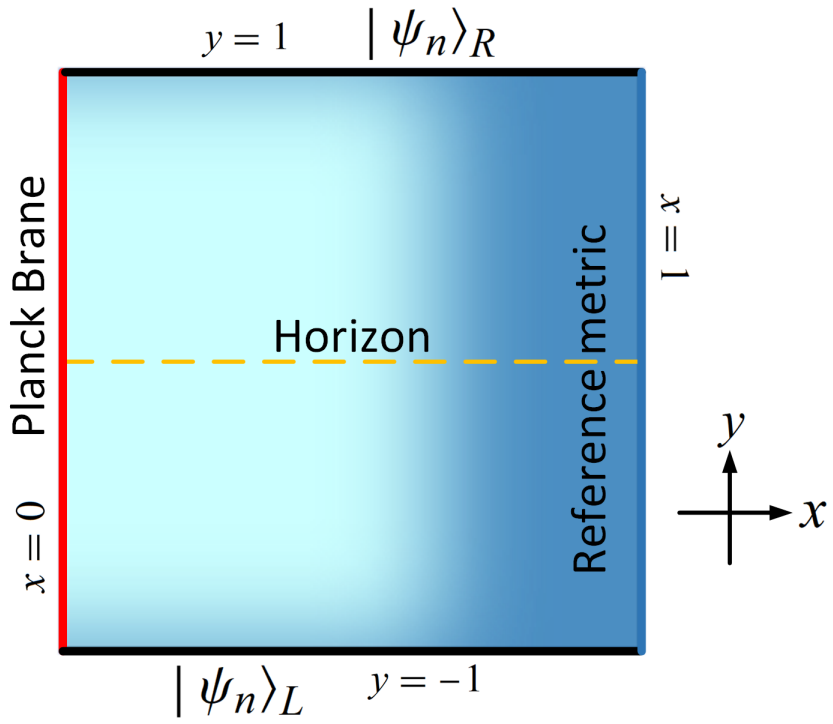

Figure 2.2: The bulk manifold $\mathcal{M}$ is in (x, y) coordinate. The yellow dashed line is the event horizon of $\mathcal{M}$, which is located at $y = 0$, and the Planck brane $\mathcal{B}$ is situated at $x = 0$, marked by the red solid line. We require $\mathcal{M} \to \widetilde{\mathcal{M}}$ as $x \to 1$ or $y \to 1$.

The numerical factors $\{K_I, q \mid I \in \{1, 2, 3, 4, 5, 6, 7\}\}$ are the function of $(x, y) \in (0, 1)^2$ can be obtained by solving (2.16). While $x \to 1$, the metric ansatz (2.19) will asymptotic to reference metric (2.17), that is, $K_1 = K_2 = K_4 = K_5 = K_6 = K_7 = 1$ and $K_3 = \cot\theta$. Because both $\mathfrak{g}$ and $\tilde{\mathfrak{g}}$ are asymptotic flat when $y \to 1$, we demand the metric ansatz (2.19) also approaches to reference metric (2.17) as $y \to 1$. Furthermore, since we impose Neumann boundary conditions for all variables, we have $\partial_y K_I|_{y=0} = 0$ and $\partial_y q|_{y=0} = 0$. To keep the Hawking temperature of $\mathfrak{g}$ to be the same as $\tilde{\mathfrak{g}}$, we require $K_1(x, 0) = K_2(x, 0)$. In the end, the plank brane is located at $x = 0$, we ask $n_\mu \xi^\mu = 0$, $K_3(0, y) = \cot\theta$ associated with (2.6) and (2.7).

Chapter 3

Time Evolution of Wormhole Area

If the reservoir CFT with finite temperature, the corresponding gravitational dual $\mathcal{M}$ is the asymptotic AdS-black brane. Particularly, while we consider $\theta_{\mathcal{B}} \to \pi/2$ limit, $\mathcal{M} \to \widetilde{\mathcal{M}}$. Hence, in the no island phase, the RT surface Γ is the wormhole path (the green lines in Fig. 2.1). This quantity is also related to the time evolution of holographic complexity [36] for computational complexity=volume (CV) conjectures. In this section, we are going to explore the time evolution of $\mathcal{A}_{\Gamma,\mathcal{I}=\{\emptyset\}}$.

3.1 Dynamics of Wormhole

Let's rewrite the Kerr-Newman metric (2.17) in Eddington–Finkelstein coordinates

$$ds^2_{\mathcal{M}} = \frac{L^2}{z^2}\Big[-dv^2\left(1-\Theta^2 g(z)\right) - 2dvdz\Theta + 2ad\psi(dz - dv\Theta g(z)) + d\psi^2\left(1+a^2 g(z)\right) + d\sigma^2_{n-1}\Big] \tag{3.1}$$

where

$$dv = dt - \frac{\Theta}{h(z)}dz \quad d\psi = d\phi - \frac{a}{h(z)}dz\,. \tag{3.2}$$

It is convenient to use the radial direction[1] λ to parameterized the extremal surface Γ

$$\mathcal{A}_{\Gamma,\mathcal{I}=\{\emptyset\}} = L^n \mathcal{A}_{\partial\Upsilon}\int_{\lambda_m}^{\lambda_{UV}} \mathcal{L}(\dot{v},\dot{z},v,z;\lambda)\,d\lambda \tag{3.3}$$

with

$$\mathcal{L}(\dot{v},\dot{z},v,z;\lambda) = \frac{1}{z^n}\sqrt{-\dot{v}^2\left(1-\Theta^2 g\left(z\right)\right) - 2\Theta\dot{v}\dot{z} - \frac{2a^2\dot{z}}{h\left(z\right)}\left(\dot{z}-\Theta g\left(z\right)\dot{v}\right) + \frac{a^2\dot{z}^2}{h\left(z\right)^2}\left(a^2 g\left(z\right)+1\right)} \tag{3.4}$$

where $z(\lambda_{UV}) = z_{UV}$ is the UV cutoff and λ_m is the turning point of z, that is , $\dot{z}(\lambda_m) = 0$. Since Lagrangian does not explicitly depend on λ in (3.3), we can choose the appropriate λ so that

$$\mathcal{L}(\dot{v},\dot{z},v,z;\lambda) = L^{n-1}\,. \tag{3.5}$$

[1]Here we assumed $\lambda \propto r^{\alpha>0} = \frac{1}{z^{\alpha>0}}$

By varying the variables v and z and applying (3.5), we obtained the equation of motion

$$\partial_\lambda \left[\frac{(1-\Theta^2 g(z))}{h(z)\, z^{2n}} \left(\dot{v} h(z) + \Theta \dot{z} \right) \right] = 0 \tag{3.6}$$

$$\partial_\lambda \left[\frac{1}{z^{2n}} \left(\Theta \dot{v} \frac{(1-\Theta^2 g(z))}{h(z)} + a^2 \dot{z} \frac{(1-(1+\Theta^2) g(z))}{h(z)^2} \right) \right] = \frac{n L^{2n-2}}{z} - \frac{\partial_z g(z)}{2 z^{2n}} \tilde{K} \tag{3.7}$$

$$\text{with} \quad \tilde{K} \equiv \Theta^2 \dot{v}^2 + 2a^2 \Theta \frac{\dot{v}\dot{z}}{h(z)^2} + \frac{a^2 \dot{z}^2}{h(z)^3} \left(a^2 + \left(\Theta^2 + 1 \right) g(z) \right) . \tag{3.8}$$

Observing (3.6), there is a constant of motion

$$E = \frac{(1-\Theta^2 g(z))}{h(z) z^{2n}} \left(\dot{v} h(z) + \Theta \dot{z} \right), \quad h(z) = 1 - g(z) \tag{3.9}$$

due to $\partial_v h(z) = 0$ in the left-hand side of (3.6). Via (3.9), we get the relation between $v(\lambda)$ and $z(\lambda)$

$$\dot{v} = \frac{E z^{2n} - \frac{(1-\Theta^2 g(z))}{h(z)} \Theta \dot{z}}{(1-\Theta^2 g(z))} . \tag{3.10}$$

Plugging (3.10) into (3.5), we obtained the equation of motion for $z(\lambda)$

$$\dot{z} = -L^{n-1} z^n h(z) \sqrt{\frac{1-\Theta^2 g(z) + E^2 L^{2-2n} z^{2n}}{(1-\Theta^2 g(z)) h(z)}} . \tag{3.11}$$

If we know the value E, form (3.11), we can determine the turning point by

$$1 - \Theta^2 g(z_m) + L^{2-2n} E^2 z_m^{2(n+1)} = 0, \quad \text{and} \quad z_m \equiv z(\lambda_m) . \tag{3.12}$$

It is convenient to measure this thermalization process by boundary time $v(\lambda_{UV}) \equiv \mathfrak{t}$, then we have $\mathfrak{t} = v(\lambda_m) + \int_{z_{UV}}^{z_m} \left(-\frac{\dot{v}}{\dot{z}} \right) dz$. Using the relation in (3.2), we get $v(\lambda_m) = \int_0^{z_m} \frac{\Theta dz}{h(z)}$. Here we conclude

$$\mathfrak{t} = \int_0^{z_m} \frac{\Theta}{h(z)} dz + \int_{z_{UV}}^{z_m} \frac{1}{h(z)} \left(\frac{E z^n}{(1-\Theta^2 g(z)) L^{n-1}} \sqrt{\frac{(1-\Theta^2 g(z)) h(z)}{1-\Theta^2 g(z) + E^2 L^{2-2n} z^{2n}}} + \Theta \right) dz . \tag{3.13}$$

Applying (3.3), (3.5) and (3.11), we can formulate

$$\mathcal{A}_{\Gamma, \mathcal{I}=\{\emptyset\}} = L^n \mathcal{A}_{\partial \Upsilon} \int_{z_{UV}}^{z_m} \frac{1}{z^n h(z)} \sqrt{\frac{(1-\Theta^2 g(z)) h(z)}{1-\Theta^2 g(z) + E^2 L^{2-2n} z^{2n}}} \, dz . \tag{3.14}$$

From (3.13) and (3.14), we obtain the derivative wormhole area with respect to the boundary time

$$\frac{d\mathcal{A}_{\Gamma,\mathcal{I}=\{\emptyset\}}}{d\mathfrak{t}} = L^n \mathcal{A}_{\partial\Upsilon} \frac{\sqrt{|1-\Theta^2 g(z_m)|}}{z_m^n} = \mathcal{A}_{\partial\Upsilon}|E|L\,. \tag{3.15}$$

For the second equality in (3.15), we have used (3.12). Here we see the additional rotation correction $\Theta \in [1,\infty)$ in (3.15). As rotating parameter a increase, so does the entanglement entropy. Note that the result (3.15) return to the charged black hole case [33, 36] as the rotating parameter a vanishes ($i.e.\Theta = 1$). We emphasize that the entanglement growth is independent of ϕ coordinate owing to the translational symmetry of spacetime, so that the ambiguity of how the increase of the radiation regions Υ is not important. The reason why area time-dependent is that wormhole itself is time-dependent.

3.2 Late Times

We suppose that the evaporation is tremendously slow such that $\mathfrak{t}_P \to \infty$. In the late times' regime, the entanglement grows linearly due to there exist the critical surface z_{mc} that a great part of the extremal surface runs along this critical surface z_{mc} [37]

$$\Delta\mathcal{A}_{\Gamma,\mathcal{I}=\{\emptyset\}} \simeq L^n \mathcal{A}_{\partial\Upsilon} v_E \mathfrak{t} \tag{3.16}$$

where the entanglement velocity

$$v_E = \frac{\sqrt{|1-\Theta^2 g(z_{mc})|}}{z_{mc}^n} \tag{3.17}$$

can be computed by finding the critical surface z_{mc}

$$\frac{d}{dz_m}\left(\frac{\sqrt{|1-\Theta^2 g(z_m)|}}{z_m^{n+1}}\right)\Bigg|_{z_m=z_{mc}} = 0 \quad \Rightarrow \quad z_{mc} = \left(\frac{2n}{m(n-1)\Theta^2}\right)^{\frac{1}{n+1}}\,. \tag{3.18}$$

Specifically, $v_E = \sqrt{\frac{n+1}{n-1}}\left(\frac{2n}{m(n-1)\Theta^2}\right)^{-\frac{n}{n+1}}$ in the Kerr case ($q=0$). We conclude that if the characteristic of Kerr-Newman black hole ($\mathcal{E}, \mathcal{Q}, \mathcal{J}$) and the spacetime dimension n are known, the entanglement velocity can be determined. For Kerr black brane, it is easy to see $v_E = 0$ at zero temperature. For RN black brane, [33] has shown some numerical results which indicate the entanglement velocity vanishes $v_E = 0$ in the extremal case.

Chapter 4

Saturation and Quantum Extremal Island

We have seen that the wormhole area will keep growing linearly (3.16) in late times until the island appears. There is an ambiguity that we do not know how big the radiation region is. Having said that, we can find the relation between the size of radiation regions and the entanglement entropy of Hawking radiation.

From [44], the relation between the Newton's constant in bulk $\mathcal{M}$ and brane $\mathcal{B}$ is

$$G_N^{(\mathcal{M})} = G_N^{(\mathcal{B})} L \int_{\pi/2}^{\theta} \csc^{n-1}(y)\, dy\,. \tag{4.1}$$

If we take $\theta_{\mathcal{B}} \to \pi/2$ limit, the Newton's constant in bulk $G_N^{(\mathcal{M})}$ is much smaller than the Newton's constant in brane $G_N^{(\mathcal{B})}$, which means the entanglement entropy in the island phase is dominated by the quantum part of (1.4) and the $\mathcal{A}_{\partial\mathcal{I}}/(4G_N^{(\mathcal{B})})$ in (2.9) is neglectable. Moreover, in a such limit, the von Neumann entropy of Hawking radiation is approximately identical to the HEE for the strip with width $2R$, *i.e.* $\mathcal{A}_{\Gamma,\mathcal{I}\neq\{\emptyset\}} \simeq 2\mathcal{A}_{strip}(\phi_R)$. We put the detail calculations in Appendix A. In this chapter, we just conclude that when island appears, the entanglement entropy of Hawking radiation in the

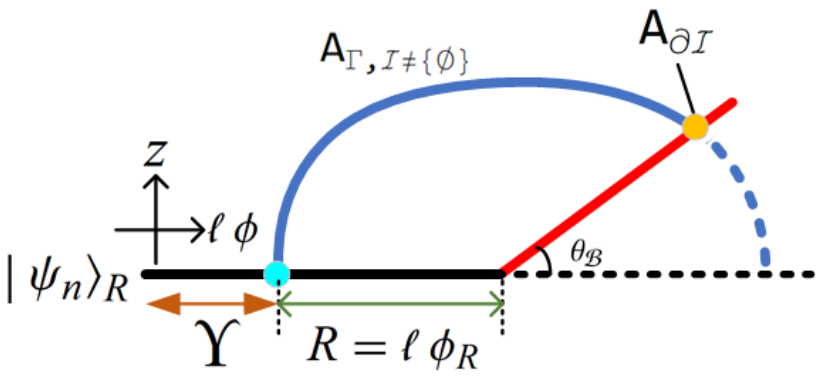

Figure 4.1: When the islands appear, the RT surface is equal to the minimal surface defect given the strip in the boundary.

small R limit [1] is

$$\Delta\mathcal{S}_\Upsilon \equiv \mathcal{S}_\Upsilon - \mathcal{S}_{\Upsilon(0)} \simeq m\frac{L^n\mathcal{A}_{\partial\Upsilon}}{4G_N^{(\mathcal{M})}}\left(\frac{n}{2}+a^2\right)\frac{\tilde{R}_1}{\tilde{R}_0^2}\phi_R^2 \tag{4.2}$$

in which $\tilde{R}_0 \equiv \frac{\sqrt{\pi}\,\Gamma\left(\frac{1}{2}+\frac{1}{2n}\right)}{\Gamma\left(\frac{1}{2n}\right)}$, $\tilde{R}_1 \equiv \frac{\sqrt{\pi}\,\Gamma\left(\frac{1}{n}\right)}{2n(n+2)\Gamma\left(\frac{1}{2}+\frac{1}{n}\right)}$ and the entanglement entropy in vacuum is

$$\mathcal{S}_{\Upsilon(0)} = \frac{L^n\mathcal{A}_{\partial\Upsilon}}{4G_N^{(\mathcal{M})}}\left(\frac{1}{\tilde{z}_{\rm UV}^{n-1}} - \frac{\tilde{R}_0^n}{(n-1)\phi_R^{n-1}}\right). \tag{4.3}$$

Also, in the large R limit[2], the leading behavior of entanglement entropy is

$$\Delta\mathcal{S}_\Upsilon \simeq \frac{L^n\mathcal{A}_{\partial\Upsilon}}{4G_N^{(\mathcal{M})}}\frac{\Theta\,\phi_R}{z_h^n}. \tag{4.4}$$

We see that, in the small R limit, the charge parameter q does not appear in the leading behavior (4.2); in the large R limit, the leading behavior of entanglement entropy is equal to the area of horizon divided by $4G_N^{(\mathcal{M})}$, which is Bekenstein-Hawking entropy. Note that, in both small and large R limits, the entanglement entropy increase as rotating parameter a increases.

[1] The intersection between the RT surface Γ and the Plank brane $\mathcal{B}$ is far from the event horizon.
[2] The intersection between the RT surface Γ and the Plank brane $\mathcal{B}$ is very close to the event horizon.

Chapter 5

Conclusions

We have analytically investigated the Page-like curve for the Kerr-Newman black brane ($k = 0$) at the semi-classical level by the holographic approach. Although to study the more realistic problem, we should consider the black hole with cosmological constant $\Lambda = 0$ and the topology of the boundary (located at $r = \infty$) is the sphere ($k = 1$), at least, there is a chance to discover pedagogically some hints about the black information paradox. Besides, we will focus the discussion on how the rotating parameter affects the von Neumann entropy of Hawking radiation.

5.1 Entanglement Growth during Thermalization

Before Page time, from (3.15), we see the rate of entanglement growth is proportional to the rotating parameter and mass parameter. In particular, in the late times, there is a great part of the wormhole along the critical surface, which leads the linear growth. There are similar properties occurs that occur in the situation that the entanglement entropy during the thermalization is discussed in [23, 24]. We discover that the entanglement velocity v_E in (3.17) is only determined by the emblackening factor $h(z)$ and the rotating parameter a, which characterizes the feature of the equilibrium state of the black brane. Notice that when the rotating parameter a increases, the entanglement velocity v_E speeds up. That means the faster the black brane rotates, the entangled Hawking particles to be radiated faster in late times.

5.2 Saturation

After Page time, the saturation entropy in weak tension limit ($\theta_{\mathcal{B}} \to \pi/2$) is approximately equal to the HEE in the cylindrical Kerr-Newman-AdS black brane by considering the shape of the subsystem in the boundary is a strip with width $2R$, and we derive the analytic results in the small and large R limits. After regularization (removing the UV divergent term), we find that the effect of rotating parameter a always come in quadratic of ϕ_R in the small R limit (4.2) and there is no charge correction in

leading behaviour. This result recovers the previous studies in [12, 13, 15–19]. Because AdS (in vacuum) is maximally symmetric spacetime, therefore the spacetime geometry felt by any observer in an inertial frame is the same. Here we see that there is no rotating parameter in vacuum (4.3) because the rotating effect vanishes in metric tensor (1.6) when $h \to 1$. In addition, if we write back the radius of the cylinder ℓ, we discover that $\Delta\mathcal{S}_\Upsilon \propto \ell^2 {\phi_R}^2$. The reason why it should be quadratic of ϕ_R is that, once we recognize the entanglement entropy $\Delta\mathcal{S}_\Upsilon$ should proportional to the area of $\partial\Upsilon$ and the energy density $\mathcal{E}$ (remember $\mathcal{E} \propto m$ in (1.10)), we are able to deduce the $\Delta\mathcal{S}_\Upsilon$ should proportional to the quadratic of ϕ_R^2 according to the dimension analysis. Note that (4.2) is valid for both extremal and non-extremal case. In the large R limit, the corrections of black brane charge q implicitly affect on z_h in (A.41). However, the corrections of a explicitly occur in the leading term while we write entanglement entropy in terms of ϕ_R (4.4). In fact, it is due to the length contraction of the event horizon in ϕ direction under Lorentz boost, that is, $\phi_R \to \phi'_R = \Theta\phi_R$. Note that both results, (4.2) and (4.4), exhibit the extensive property of entanglement entropy.

5.3 Quantum Information during Evaporation

Remember the entanglement entropy is a measurement that quantifies how much entanglement between Υ and Υ^c. Before the observation, we can regard the entanglement entropy $\Delta\mathcal{S}_\Upsilon$ as the information from Υ^c is owned by the observer stand in Υ, and the observer in Υ is not accessible to Υ^c. While $\Delta\mathcal{S}_\Upsilon$ increases, that means we stand in radiation regions Υ gain the information from black hole regions, and information we gained reach maximum as the system reach equilibrium. Our results indicate that the final equilibrium state is only dependent on the thermodynamic variables of the grand canonical ensemble $(\phi_R, \mathcal{E}, \mathcal{Q}, \mathcal{J})$, no matter what the initial state we prepare.

Appendices

Appendix A

HEE in Cylindrical Kerr-Newman Black Brane

Because, in the weak tension limit, the entanglement entropy of Hawking radiation is same as the HEE for the strip while our holographic system reaches saturation. In this chapter, we are going to provide the detail calculations of HEE for stip in cylindrical Kerr-Newman black brane.

A.1 Integration form of Area and Boundary

In the following calculation, we will consider a strip boundary defined by

$$\Sigma \equiv \left\{ x_i, \phi \middle| x_i \in \left[-\frac{W}{2}, \frac{W}{2} \right], \phi \in \left[-\phi_R, \phi_R \equiv \frac{R}{\ell} \right] \right\}, \tag{A.1}$$

where ℓ is the radius of the cylinder. For simplicity, we let ℓ be 1. The associated extremal surface Γ in the bulk can be parameterized by $\xi^i = (\phi, \vec{x})$ with embedding $y^\mu(\xi^i) = (z(\phi), \phi, \vec{x})$, and the induced metric is

$$\gamma_{ij} = g_{\mu\nu} \frac{\partial y^\mu}{\partial \xi^i} \frac{\partial y^\nu}{\partial \xi^j}. \tag{A.2}$$

Since the bulk metric is independent of the coordinate ϕ, the extremal surface should have symmetry with respect to ϕ. Therefore, it is convenient to let the tip of the extremal surface is at $z_b = z(\phi = 0)$.

Moreover, one should introduce the UV cutoff $z_{\rm UV}$ for regularization of the area of the extremal surface near the boundary $\phi = \phi_R$, i.e. $z(\phi_R) = 0$. Therefore, the area of

the extremal surface $\mathcal{A}_\Gamma$ is

$$\begin{aligned}\mathcal{A}_\Gamma &= 2\int_0^{\phi_R-\phi(z_{\rm UV})} d\phi \int_{-\frac{W}{2}}^{\frac{W}{2}} d\vec{x}\,\sqrt{\det\gamma_{ij}} \\ &= 2W^{n-1}L^n\int_0^{\phi_R-\phi(z_{\rm UV})} d\phi\,\frac{1}{z^n}\sqrt{-a^2h(z)+\Theta^2+\frac{\dot{z}^2}{h(z)}} \\ &\equiv L^n\mathcal{A}_{\partial\Sigma}\int_0^{\phi_R-\phi(z_{\rm UV})} d\phi\,\mathcal{L}(\dot{z},z;\phi),\end{aligned} \tag{A.3}$$

where $\mathcal{A}_{\partial\Sigma}=2W^{n-1}$, $\dot{z}=\partial z/\partial\phi$ and the corresponding Lagrangian is

$$\mathcal{L}(\dot{z},z;\phi)=\frac{1}{z^n}\sqrt{\frac{\dot{z}^2}{h(z)}+\mathcal{C}(z)},\qquad \mathcal{C}(z)\equiv\Theta^2-a^2h(z)=1+a^2g(z). \tag{A.4}$$

Consequently, the associated Hamiltonian is

$$\mathcal{H}=\frac{\partial\mathcal{L}}{\partial\dot{z}}\dot{z}-\mathcal{L}=-\frac{\mathcal{C}(z)}{z^{2n}\mathcal{L}}. \tag{A.5}$$

Since the Hamiltonian does not explicitly depend on ϕ implying that the $\mathcal{H}$ is a constant of motion along ϕ direction, in the other words, there is a translational symmetry along ϕ direction. Because of translational symmetry, it enables us to compute the value of Hamiltonian by evaluating at tip of minimal surface $z=z_b$ such that $\dot{z}=0$

$$\mathcal{H}(z=z_b)=-\frac{\sqrt{\mathcal{C}(z_b)}}{z_b^n}<0. \tag{A.6}$$

From (A.5), we can obtain the equation of motion (EoM) for $z(\phi)$ to minimize the area $\mathcal{A}_\Gamma$

$$\dot{z}=\mp\frac{\mathcal{C}(z)\sqrt{h(z)}\sqrt{1-\frac{z^{2n}\mathcal{C}(z_b)}{z_b^{2n}\mathcal{C}(z)}}}{(-\mathcal{H})z^n},\qquad \forall\phi\gtrless 0. \tag{A.7}$$

The equation (A.7) shows that the shape of the minimal surface is symmetric. Therefore, we are able to rewrite the area formula

$$\begin{aligned}\mathcal{A}_\Gamma &= L^n\mathcal{A}_{\partial\Sigma}\int_{z_{\rm UV}}^{z_b}\mathcal{L}(\dot{z},z;\phi)\frac{1}{(-\dot{z})}\,dz \\ &= L^n\mathcal{A}_{\partial\Sigma}\int_{z_{\rm UV}}^{z_b}\frac{1}{z^n\sqrt{h(z)}\sqrt{1-\frac{z^{2n}\mathcal{C}(z_b)}{z_b^{2n}\mathcal{C}(z)}}}\,dz.\end{aligned} \tag{A.8}$$

Also, we can obtain the relation between ϕ_R and z_b through

$$\phi_R=\int_0^{z_b}\frac{1}{\dot{z}}\,dz=\int_0^{z_b}\frac{(-\mathcal{H})z^n}{\mathcal{C}(z)\sqrt{h(z)}\sqrt{1-\frac{z^{2n}\mathcal{C}(z_b)}{z_b^{2n}\mathcal{C}(z)}}}\,dz. \tag{A.9}$$

It is difficult to compute the integration (A.8) explicitly. We are going to focus on two specific limits of small and large values of R.

A.2 Entanglement Entropy in the Small R Limit

To evaluate the area of the extremal surface in the small or large R limits, it is convenient to introduce new variables as

$$\eta = \frac{z_b}{z_h}, \qquad u = \frac{z}{z_b}, \tag{A.10}$$

and then

$$\mathcal{C}(u) = 1 + a^2 g(u), \qquad g(u) = \eta^{n+1} u^{n+1} \left[1 + q^2 z_h^{2n} (1 - \eta^{n-1} u^{n-1})\right]. \tag{A.11}$$

In the small R limit, the tip of the extremal surface z_b is far away from the position of the horizon z_h, that is, $0 < z_b \ll z_h$ or $0 < \eta \ll 1$. Thus we are going to find the leading behavior of area (A.8) and ϕ_R (A.9) in the limit $\eta \to 0$, respectively.

A.2.1 Relation Between ϕ_R and η

Expanding the integrand of (A.9) in the small η, we got ($n \geq 2$)

$$\phi_R = (-\mathcal{H}) \int_0^1 \left[C_{n+1}(u)\eta^{n+1} + C_{2n+2}(u)\eta^{2n+2} + O\left(\eta^{3n+1}\right)\right] du, \tag{A.12}$$

where the first two leading orders are

$$C_{n+1}(u) = \frac{u^n z_h^{n+1}}{\sqrt{1-u^{2n}}}, \qquad C_{2n+2}(u) = C^{(1)}_{2n+2}(u) + C^{(2)}_{2n+2}(u), \tag{A.13}$$

$$C^{(1)}_{2n+2}(u) = \frac{1-2a^2}{2} z_h^{n+1}(q^2 z_h^{2n} + 1) \frac{u^{2n+1}}{\sqrt{1-u^{2n}}}, \tag{A.14}$$

$$C^{(2)}_{2n+2}(u) = \frac{a^2}{2} z_h^{n+1}(q^2 z_h^{2n} + 1) \frac{u^{3n} - u^{4n+1}}{(1-u^{2n})^{3/2}}. \tag{A.15}$$

We employed the Euler integral of the first kind [1] to evaluate the integration

$$\int_0^1 C_{n+1}(u)\,du = \tilde{R}_0 z_h^{n+1}, \tag{A.16}$$

$$\int_0^1 C^{(1)}_{2n+2}(u)\,du = \left(1-2a^2\right)\left(q^2 z_h^{2n}+1\right)\tilde{R}_1 z_h^{n+1}, \tag{A.17}$$

$$\int_0^1 C^{(2)}_{2n+2}(u)\,du = \frac{a^2(n+1)}{2n}(q^2 z_h^{2n}+1)\left(4\tilde{R}_1-\tilde{R}_0\right) z_h^{n+1}. \tag{A.18}$$

where $\tilde{R}_0 \equiv \frac{\sqrt{\pi}\,\Gamma\left(\frac{1}{2}+\frac{1}{2n}\right)}{\Gamma\left(\frac{1}{2n}\right)}$ and $\tilde{R}_1 \equiv \frac{\sqrt{\pi}\,\Gamma\left(\frac{1}{n}\right)}{2n(n+2)\Gamma\left(\frac{1}{2}+\frac{1}{n}\right)}$. Note that the divergences of both two "beta-functions"-like contributions in (A.18) indeed cancel out to give a finite result. To compute (A.15), we need to convert $(1-u^{2n})^{-3/2}$ to summation form

$$\begin{aligned}\int_0^1 \frac{u^{3n}-u^{4n+1}}{(1-u^{2n})^{3/2}}du &= \sum_{j=0}^{\infty}\frac{2\Gamma\left(j+\frac{3}{2}\right)}{\sqrt{\pi}\,\Gamma(j+1)}\int_0^1 u^{2nj+3n}(1-u^{n+1})\,du \\ &= \frac{n+1}{n}\left(4\tilde{R}_1-\tilde{R}_0\right).\end{aligned} \tag{A.19}$$

On top of that, the Hamiltonian in the small η limit looks like

$$\mathcal{H} = -\frac{1}{z_h^n\eta^n} - \frac{a^2}{2z_h^n}(q^2 z_h^{2n}+1)\eta + \frac{1}{2}a^2q^2 z_h^n\eta^n + O(\eta^{n+2}). \tag{A.20}$$

Plugging the results (A.16, A.17, A.18) and (A.20) into (A.12), we found the ϕ_R in the small η limit

$$\phi_R = \tilde{R}_0 z_h\eta + \left[\tilde{R}_1 + \frac{2a^2}{n}\left(\tilde{R}_1 - \frac{\tilde{R}_0}{4}\right)\right](q^2 z_h^{2n}+1)z_h\eta^{n+2} + O(\eta^{2n+1}). \tag{A.21}$$

In Schwarzschild case [19], $\phi_R = z_h\sum_{j=0}^{\infty}\tilde{R}_j\eta^{j(n+1)+1}$ with $\tilde{R}_j = \frac{1}{2n}\frac{\Gamma\left(j+\frac{1}{2}\right)\Gamma\left(\frac{1}{2}+\frac{1}{2n}+\frac{j(n+1)}{2n}\right)}{\Gamma(j+1)\Gamma\left(1+\frac{1}{2n}+\frac{j(n+1)}{2n}\right)}$. It is easy to see that the correction in (A.21) due to rotation a and charge parameter q.

A.2.2 Area

Now we move on to the integration of the area. First, we expand the integrand at $\eta \to 0$ limit

$$\mathcal{A}_\Gamma = L^n\mathcal{A}_{\partial\Sigma}\int_0^1\left[\tilde{C}_{-n+1}(u)\eta^{-n+1} + \tilde{C}_2(u)\eta^2 + O(\eta^{n+1})\right]du, \tag{A.22}$$

[1] The integration form of beta function is

$$\int_0^1 x^{\mu-1}(1-x^\lambda)^{\nu-1}\,dx = \frac{B(\mu/\lambda,\nu)}{\lambda}, \quad \forall\ \mu>0,\ \nu>0,\ \lambda>0,$$

and $B\left(\frac{\mu}{\lambda},\nu\right) = \frac{\Gamma(\mu/\lambda)\Gamma(\nu)}{\Gamma(\mu/\lambda+\nu)}$,

where

$$\tilde{C}_{-n+1}(u) = \frac{1}{z_h^{n-1}u^n\sqrt{1-u^{2n}}}, \qquad \tilde{C}_2(u) = \tilde{C}_2^{(1)}(u) + \tilde{C}_2^{(2)}(u), \tag{A.23}$$

$$\tilde{C}_2^{(1)}(u) = \frac{1}{2z_h^{n-1}}(q^2z_h^{2n}+1)\frac{u}{\sqrt{1-u^{2n}}}, \tag{A.24}$$

$$\tilde{C}_2^{(2)}(u) = \frac{a^2}{2z_h^{n-1}}(q^2z_h^{2n}+1)\frac{u^n-u^{2n+1}}{(1-u^{2n})^{3/2}}. \tag{A.25}$$

It is a little different from the integration of ϕ_R. Here the leading order contribution is divergent due to the divergence of integrant at $u = 0$. By introducing the UV cut-off $u_{\rm UV} = z_{\rm UV}/z_b$, and the relation

$$\frac{1}{n-1} - \int_0^1 \frac{1}{u^n}\left(\frac{1}{\sqrt{1-u^{2n}}} - 1\right) du = \frac{\sqrt{\pi}\,\Gamma\left(\frac{1}{2}+\frac{1}{2n}\right)}{(n-1)\Gamma\left(\frac{1}{2n}\right)}. \tag{A.26}$$

The divergent term comes from (A.27), and we have the ability to extract the divergent term

$$\begin{aligned} z_h^{n-1}\int_0^1 \tilde{C}_{-n+1}(u)\,du &= \int_{u_{\rm UV}}^1 \frac{du}{u^n} + \int_0^1 \frac{du}{u^n}\left(\frac{1}{\sqrt{1-u^{2n}}} - 1\right) \\ &= \frac{1}{n-1}\left(\frac{1}{u_{\rm UV}}\right)^{n-1} - \frac{\tilde{R}_0}{(n-1)}. \end{aligned} \tag{A.27}$$

There other two integrations are similar to the calculation of ϕ_R, it is easy to get the answers

$$\int_0^1 \tilde{C}_2^{(1)}(u)\,du = \frac{q^2z_h^{2n}+1}{2z_h^{n-1}}(n+2)\tilde{R}_1, \tag{A.28}$$

$$\int_0^1 \tilde{C}_2^{(2)}(u)\,du = \frac{a^2}{2nz_h^{n-1}}(q^2z_h^{2n}+1)\left(2(n+2)\tilde{R}_1 - \tilde{R}_0\right). \tag{A.29}$$

Plugging the results (A.27), (A.28) and (A.29) into (A.22), we obtained the area of the extremal surface in terms of η in the small R limit

$$\frac{\mathcal{A}_\Gamma}{L^n\mathcal{A}_{\partial\Sigma}} = \frac{1}{\tilde{z}_{\rm UV}^{n-1}} - \frac{\tilde{R}_0}{n-1}z_h^{1-n}\eta^{1-n} + (q^2z_h^{2n}+1)\frac{n+2}{2}\left[\tilde{R}_1 + \frac{a^2}{n}\left(2\tilde{R}_1 - \frac{\tilde{R}_0}{n+2}\right)\right] z_h^{1-n}\eta^2 + O(\eta^{n+1}), \tag{A.30}$$

where $\tilde{z}_{\rm UV} = (n-1)^{1/(n-1)}z_{\rm UV}$. Since (A.21) tells us the relation between η and ϕ_R, we can write down the entanglement entropy in terms of ϕ_R

$$\delta\mathcal{S}_\Sigma \equiv \mathcal{S}_\Sigma - \mathcal{S}_{\Sigma(0)} \simeq L^n\mathcal{A}_{\partial\Sigma}\frac{m}{4G_N}\left(\frac{n}{2}+a^2\right)\frac{\tilde{R}_1}{\tilde{R}_0^2}\phi_R^2. \tag{A.31}$$

where $4G_N\mathcal{S}_{\Sigma(0)}/(L^n\mathcal{A}_{\partial\Sigma}) = \frac{1}{\tilde{z}_{\rm UV}^{n-1}} - \frac{\tilde{R}_0^n}{(n-1)\phi_R^{n-1}}$ is the area of the extremal surface in vacuum.

A.3 Entanglement Entropy in the Large R Limit

In the large R limit, $\eta \to 1$, the tip of the extremal surface should vary close to the event horizon, namely

$$z_b = z_h(1-\epsilon), \qquad \text{for } 0 < \epsilon \ll 1. \tag{A.32}$$

Moreover, we believe that the leading term of the "regularized" extremal surface, i.e. after removing the UV divergent, in the large R limit is almost equal to the area of even horizon, therefore we have

$$\mathcal{A}_\Gamma\Big|_{\text{reg.}} \simeq \frac{\Theta\,\phi_R}{z_h}\frac{L^n\mathcal{A}_{\partial\Sigma}}{z_h^{n-1}} \quad \Rightarrow \quad \frac{\mathcal{A}_\Gamma}{L^n\mathcal{A}_{\partial\Sigma}} - \frac{1}{\tilde{z}_{\text{UV}}^{n-1}} \simeq \frac{\Theta\,\phi_R}{z_h^n}. \tag{A.33}$$

Our goal is to find the leading behavior of (A.8) and (A.9) in the large R expansion by assuming the corresponding integrations are dominated by the region $z \simeq z_b$ in the large R limit. We can execute the integration after expanding the integrand in IR regions. This approximation is valid to find the leading term which can be justified by checking the results in the small a and q limits. In this thesis, we only show how to deal with the integration (A.9) in the large R limit. It is easy to verify (A.33) by using the same method to calculate the integration (A.8).

Observing that the leading term of the emblackening factor $h(z)$ near horizon $z = z_h$ for non-extremal is proportional to the black brane temperature by (1.14), and it is proportional to the second derivative of $h(z)$ when black brane is extremal, i.e

$$h(z) \simeq p z_h^q (1-\eta u)^q \quad \text{where} \quad \begin{cases} q=1, \;\; p = 4\pi\Theta T & \text{at } T \neq 0 \\ q=2, \;\; p = \frac{n(n+1)}{z_h^2} & \text{at } T = 0 \end{cases}. \tag{A.34}$$

Here we do the coordinate transformation by (A.10). Recognizing that the main contribution of integration is from the IR region, we can find the leading behavior by finding the expansion of integrand at $u = 1$ and then carry out the integration. More precisely, we have

$$\mathcal{C}(u) = \mathcal{C}(1) + O(u-1) = \left[\Theta^2 + O(u-1)\right] + O(\epsilon), \quad \mathcal{C}(1) = \Theta^2 + O(\epsilon), \tag{A.35}$$

and

$$1 - \frac{z^{2n}\mathcal{C}(z_b)}{z_b^{2n}\mathcal{C}(z)} = 1 - u^{2n}\frac{\mathcal{C}(1)}{\mathcal{C}(u)} = \left\{r\,(1-u) + O\left[(u-1)^2\right]\right\} + O(\epsilon) \tag{A.36}$$

where

$$r = 2n + \frac{a^2\partial_u h(u)}{\Theta^2} = 2n - 4\pi z_h T\frac{a^2}{\Theta} + O(\epsilon)\,. \tag{A.37}$$

Note that we have ignored the order $O(\epsilon)$ in (A.36). You can convince yourself by considering the order $O(\epsilon)$ in (A.36) and integrating it, and find that the $O(\epsilon)$ in (A.36) does not contribute to the leading behavior of ϕ_R. After doing so, via (A.34), (A.35),

(A.36) and (A.37), we obtain

$$\phi_R \simeq \frac{z_b}{\sqrt{p r z_h^q \Theta}} \int_0^1 \frac{1}{(1-\eta u)^{\frac{q}{2}} \sqrt{1-u}}\, du\,. \tag{A.38}$$

To deal with the integration (A.38), we applied the binomial identity

$$\frac{1}{(1-\eta u)^{\frac{q}{2}}} = \sum_{j=0}^{\infty} \binom{-\frac{q}{2}}{j} (-1)^j \eta^j u^j\,, \tag{A.39}$$

then the integration (A.38) becomes Euler's integral

$$\phi_R \simeq \frac{z_h}{\sqrt{p r z_h^q \Theta}} \sum_{j=0}^{\infty} \binom{-\frac{q}{2}}{j} \frac{\sqrt{\pi}\Gamma(j+1)}{\Gamma\left(j+\frac{3}{2}\right)} (-1)^j \eta^j = \frac{2 z_h}{\sqrt{p r z_h^q \Theta}}\, {}_2F_1\left(1, \frac{q}{2}; \frac{3}{2}; \eta\right)\,. \tag{A.40}$$

The summation in (A.40) is exactly equal to the hypergeometric function.[2] Hence, for finite temperature, (A.40) becomes

$$\phi_R \simeq -\frac{z_h \ln \epsilon}{\sqrt{8\pi n \Theta z_h T}} \tilde{f}(a,q), \tag{A.41}$$

where

$$\tilde{f}(a,q) \equiv \frac{\sqrt{2n}}{\sqrt{2n + a^2(n-1)(1+q^2 z_h^{2n})}} \simeq \frac{\sqrt{2n}}{\sqrt{2n - 4\pi z_h T \frac{a^2}{\Theta}}}. \tag{A.42}$$

Note that the rotation-charge couple $\tilde{f}(a,q)$ has a property $\tilde{f}(0,q) = 1$. For zero temperature, we concluded that

$$\phi_R \simeq \frac{\pi z_h}{n\Theta\sqrt{2(n+1)\epsilon}}. \tag{A.43}$$

Here we have used (A.32) to convert η to ϵ. It is easy to check that our results (A.41) and (A.43) are consistent with [15–18, 21].

[2] The hypergeometric function is defined by

$${}_2F_1(a,b;c;z) \equiv \sum_{j=0}^{\infty} \frac{(a)_j (b)_j}{(c)_j} \frac{z^j}{j!}$$

where

$$(q)_j \equiv \frac{\Gamma(q+j)}{\Gamma(q)}$$

.

References

[1] A. Almheiri, R. Mahajan, J. Maldacena and Y. Zhao, "*The Page curve of Hawking radiation from semiclassical geometry*," *JHEP* **03**, 149 (2020) [arXiv:1908.10996 [hep-th]].

[2] G. 't Hooft, "*Dimensional reduction in quantum gravity*," *Conf. Proc. C* **930308**, 284-296 (1993) [arXiv:gr-qc/9310026 [gr-qc]].

[3] L. Susskind, "*The World as a hologram*," *J. Math. Phys.* **36**, 6377-6396 (1995) [arXiv:hep-th/9409089 [hep-th]].

[4] J. M. Maldacena, "*The Large N limit of superconformal field theories and supergravity*," *Int. J. Theor. Phys.* **38**, 1113-1133 (1999) [arXiv:hep-th/9711200 [hep-th]].

[5] S. S. Gubser, I. R. Klebanov and A. M. Polyakov, "*Gauge theory correlators from noncritical string theory*," *Phys. Lett. B* **428**, 105-114 (1998) [arXiv:hep-th/9802109 [hep-th]].

[6] E. Witten, "*Anti-de Sitter space and holography*," *Adv. Theor. Math. Phys.* **2**, 253-291 (1998) [arXiv:hep-th/9802150 [hep-th]].

[7] S. Ryu and T. Takayanagi, "*Holographic derivation of entanglement entropy from AdS/CFT*," *Phys. Rev. Lett.* **96**, 181602 (2006) [arXiv:hep-th/0603001 [hep-th]].

[8] S. Ryu and T. Takayanagi, "*Aspects of Holographic Entanglement Entropy*," *JHEP* **08**, 045 (2006) [arXiv:hep-th/0605073 [hep-th]].

[9] T. Nishioka, S. Ryu and T. Takayanagi, "*Holographic Entanglement Entropy: An Overview*," *J. Phys. A* **42**, 504008 (2009) [arXiv:0905.0932 [hep-th]].

[10] T. Takayanagi, "*Entanglement Entropy from a Holographic Viewpoint*," *Class. Quant. Grav.* **29**, 153001 (2012) [arXiv:1204.2450 [gr-qc]].

[11] M. Rangamani and T. Takayanagi, "*Holographic Entanglement Entropy*," *Lect. Notes Phys.* **931**, pp.1-246 (2017) [arXiv:1609.01287 [hep-th]].

[12] J. Bhattacharya, M. Nozaki, T. Takayanagi and T. Ugajin, "*Thermodynamical Property of Entanglement Entropy for Excited States*," *Phys. Rev. Lett.* **110**, no.9, 091602 (2013) [arXiv:1212.1164 [hep-th]].

[13] H. Nadi, B. Mirza, Z. Sherkatghanad and Z. Mirzaiyan, "*Holographic entanglement first law for $d + 1$ dimensional rotating cylindrical black holes*," *Nucl. Phys. B* **949**, 114822 (2019) [arXiv:1904.11344 [gr-qc]].

[14] P. Caputa, V. Jejjala and H. Soltanpanahi, "*Entanglement entropy of extremal BTZ black holes*," *Phys. Rev. D* **89**, no.4, 046006 (2014) [arXiv:1309.7852 [hep-th]].

[15] W. Fischler and S. Kundu, "*Strongly Coupled Gauge Theories: High and Low Temperature Behavior of Non-local Observables*," *JHEP* **05**, 098 (2013) [arXiv:1212.2643 [hep-th]].

[16] P. Chaturvedi, V. Malvimat and G. Sengupta, "*Entanglement thermodynamics for charged black holes*," *Phys. Rev. D* **94**, no.6, 066004 (2016) [arXiv:1601.00303 [hep-th]].

[17] S. Kundu and J.F. Pedraza, "*Aspects of Holographic Entanglement at Finite Temperature and Chemical Potential*," *JHEP* **08** 177 (2016) [arXiv:1602.07353 [hep-th]].

[18] S. Karar, D. Ghorai and S. Gangopadhyay, "*Holographic entanglement thermodynamics for higher dimensional charged black hole*," *Nucl. Phys. B* **938**, 363-387 (2019) [arXiv:1810.08037 [hep-th]].

[19] A. Saha, S. Gangopadhyay and J. P. Saha, "*Holographic entanglement entropy and generalized entanglement temperature*," *Phys. Rev. D* **100**, no.10, 106008 (2019) [arXiv:1906.03159 [hep-th]].

[20] V. E. Hubeny, "*Extremal surfaces as bulk probes in AdS/CFT*," *JHEP* **07**, 093 (2012) [arXiv:1203.1044 [hep-th]].

[21] H. Liu and M. Mezei, "*Probing renormalization group flows using entanglement entropy*," *JHEP* **01**, 098 (2014) [arXiv:1309.6935 [hep-th]].

[22] V. E. Hubeny, M. Rangamani and T. Takayanagi, "*A Covariant holographic entanglement entropy proposal*," *JHEP* **07**, 062 (2007) [arXiv:0705.0016 [hep-th]].

[23] H. Liu and S. J. Suh, "*Entanglement Tsunami: Universal Scaling in Holographic Thermalization*," *Phys. Rev. Lett.* **112**, 011601 (2014) [arXiv:1305.7244 [hep-th]].

[24] H. Liu and S. J. Suh, "*Entanglement growth during thermalization in holographic systems*," *Phys. Rev. D* **89**, 066012 (2014) [arXiv:1311.1200 [hep-th]].

[25] P. Caputa, G. Mandal and R. Sinha , "*Dynamical entanglement entropy with angular momentum and U(1) charge*," *JHEP* **11** 052 (2013) [arXiv:1306.4974 [hep-th]].

[26] P. C. Sun, D.-S. Lee and C. P. Yeh, "*Holographic approach to thermalization in general anisotropic theories*," *JHEP* **03**, 164 (2021) [arXiv:2011.02716 [hep-th]].

[27] T. Faulkner, A. Lewkowycz and J. Maldacena , "*Quantum corrections to holographic entanglement entropy*," *JHEP* **11** 074 (2013) [arXiv:1307.2892 [hep-th]].

[28] N. Engelhardt and A. C. Wall, "*Quantum Extremal Surfaces: Holographic Entanglement Entropy beyond the Classical Regime*," *JHEP* **01** 073 (2015) [arXiv:1408.3203 [hep-th]].

[29] G. Penington, "*Entanglement Wedge Reconstruction and the Information Paradox*," *JHEP* **09** 002 (2020) [arXiv:1905.08255 [hep-th]].

[30] A. Almheiri, N. Engelhardt, D. Marolf and H. Maxfield,"*The entropy of bulk quantum fields and the entanglement wedge of an evaporating black hole*," *JHEP* **12** 063 (2019) [arXiv:1905.08762 [hep-th]].

[31] A. Almheiri, R. Mahajan and J. Maldacena, "*Islands outside the horizon*," [arXiv:1910.11077 [hep-th]].

[32] A. Almheiri, R. Mahajan and J. E. Santos, "*Entanglement islands in higher dimensions*," *SciPost Phys.* **9** 1, 001 (2020) [arXiv:1911.09666 [hep-th]].

[33] Y. Ling, Y. Liu and Z.-Y. Xian, "*Island in Charged Black Holes*," *JHEP* **03** 251 (2021) [arXiv:2010.00037 [hep-th]].

[34] H.-Z. Chen, R. C. Myers, D. Neuenfeld, I. A. Reyes and J. Sandor, "*Quantum Extremal Islands Made Easy, Part I: Entanglement on the Brane*," *JHEP* **10** 166 (2020) [arXiv:2006.04851 [hep-th]].

[35] H.-Z. Chen, R. C. Myers, I. A. Reyes and J. Sandor, "*Quantum Extremal Islands Made Easy, Part II: Black Holes on the Brane*," *JHEP* **12** 025 (2020) [arXiv:2010.00018 [hep-th]].

[36] D. Carmi, S. Chapman, H. Marrochio, R. C. Myers and S. Sugishita, "*On the Time Dependence of Holographic Complexity*," *JHEP* **11** 188 (2017) [arXiv:1709.10184 [hep-th]].

[37] T. Hartman and J. Maldacena, "*Time evolution of entanglement entropy from black hole interiors*," *JHEP* **05** 014 (2013) [arXiv:1303.1080 [hep-th]].

[38] A. M. Awad, "*Higher dimensional charged rotating solutions in (A)dS spacetimes*," *Class. Quant. Grav.* **20**, 2827-2834 (2003) [arXiv:hep-th/0209238 [hep-th]].

[39] M. H. Dehghani and A. Khodam-Mohammadi, "*Thermodynamics of a $d-$dimensional charged rotating black brane and the AdS/CFT correspondence*," *Phys. Rev. D* **67**, 084006 (2003) [arXiv:0212126 [hep-th]].

[40] T. Takayanagi, "*Holographic Dual of a Boundary Conformal Field Theory*," *Phys. Rev. Lett.* **107**, 101602 (2011) [arXiv:1105.5165 [hep-th]].

[41] M. Fujita, T. Takayanagi and E. Tonni, "*Aspects of AdS/BCFT*," *JHEP* **11** 043 (2011) [arXiv:1108.5152 [hep-th]].

[42] C.-S Chu and R.-X Miao, "*Anomalous Transport in Holographic Boundary Conformal Field Theories*," *JHEP* **07** 005 (2018) [1804.01648 [hep-th]].

[43] T. Nishioka, "*Entanglement entropy: holography and renormalization group*," *Rev. Mod. Phys.* **90**, 035007 (2018). [arXiv:1801.10352 [hep-th]].

[44] R.-X Miao, "*An Exact Construction of Codimension two Holography*," *JHEP* **01** 150 (2021) [arXiv:2009.06263 [hep-th]].